ELSEVIER

Materials Science and Engineering A334 (2002) 6–10

MATERIALS SCIENCE & ENGINEERING A

www.elsevier.com/locate/msea

Simulation of γ-hydride precipitation in bi-crystalline zirconium under uniformly applied load

X.Q. Ma [a], S.Q. Shi [a,*], C.H. Woo [a], L.Q. Chen [b]

[a] *Department of Mechanical Engineering, The Hong Kong Polytechnic University, Hung Hom, Kowloon, Hong Kong*
[b] *Department of Materials Science and Engineering, Pennsylvania State University, University Park, PA 16802, USA*

Received 11 June 2001

Abstract

The morphology evolution of γ-hydride precipitation and growth in a zirconium bi-crystal was simulated using a phase field kinetic model. The effects of grain boundary and uniformly applied load were studied. The temporal evolution of the spatially dependent field variables is determined by numerically solving the time-dependent Ginzburg–Landau equations for the structural variables and the Cahn–Hilliard diffusion equation for the concentration variable. It is demonstrated that nucleation density of the hydride at the grain boundary increases as compared to the bulk and favorable hydride precipitation at the grain boundary become weaker when an external load is applied. The result also showed that hydrides will grow in those habit planes that are near the perpendicular direction of the applied tensile load.

Keywords: Computer simulation; Zirconium hydride; Bi-crystal; Phase-field kinetic model; Morphology evolution

1. Introduction

The mechanical properties of most materials strongly depend on their phase composition and distribution. Phase transformation often causes the change of their properties. The phase-field kinetic model is an effective model in describing the morphological evolution during phase transformation. It has been successfully applied to study the morphology of the second phase precipitation in many materials [1–5].

In this work, γ-hydride precipitation in a bi-crystal zirconium with and without uniformly applied tensile load is studied. Zirconium is a structural material in nuclear power industry owing to its combination of good mechanical properties, excellent corrosion resistance and low neutron absorption cross-section. However, it often works under hot water environment. Zirconium will gradually pick up hydrogen from the hot water environment during service. When hydrogen concentration reaches a certain level, zirconium hydride will form. Since the brittleness of the hydride, the mechanical properties of the material will degrade, and fracture may initiate at the hydrides. It is believed that the critical conditions for fracture initiation at hydrides are controlled by the morphology and microstructure of hydride precipitates in zirconium [6–9].

The morphology of γ-hydride in zirconium and zirconium alloy were studied by Baily [10], Roy and Jacqes [11] and Bradbrook [12] et al. using TEM. They observed a habit plane of {1010} type in zirconium and needle-like hydrides growing in ⟨1120⟩ directions. Favorable precipitation of γ-hydride at the grain boundary in polycrystalline zirconium was also reported [10]. It has been observed that stress plays an important role in the morphology of hydrides. Effect of tensile stress on hydride orientation has been studied experimentally by Walter [13], Bayark [14] and Marchel [15] et al. The results show that in zirconium, the tensile stress tend to change the habit plane in such fashion that the hydrides orient perpendicular to the tensile stress and that some critical stress might be necessary in order for the hydride to reorient itself.

However it can be very expensive to study experimentally the morphological evolution of hydride precipitates in irradiated materials because of the cost involved for irradiation protection. Unfortunately, such

* Corresponding author. Tel.: +852-2766-7821; fax: +852-2365-4703.
E-mail address: mmsqshi@polyu.edu.hk (S.Q. Shi).

0921-5093/02/$ - see front matter
PII: S0921-5093(01)01770-1

expensive test is still the only way to study the evolution of hydride morphology in irradiated materials. Computational methods in materials science have advanced significantly in recent years [16]. It is now possible to apply computer simulation to acquire characteristics of hydride precipitation pattern quite accurately, or to have better understanding of the mechanism and to predict the properties and morphology of new phases.

A two-dimensional γ-hydride precipitation under an applied load in a zirconium single crystal has been investigated by the authors [17] using a phase-field model based on the elasticity theory of Khachaturyan [18]. The morphological evolution process of this system is in well accordance with the experimental observation [10].

However, most engineering materials are polycrystalline materials and grain boundaries may play significant role in morphology evolution. Effect of applied load in these systems should also be studied. It should be noted that microstructure evolution during martensitic transformation in polycrystals have been studied recently using a phase-field model [19]. In this report, γ-hydride precipitation in a bi-crystalline zirconium is considered. The effects of grain boundary and uniformly applied load are discussed.

2. Phase field approach

Zirconium has a hexagonal close-packed structure. The needle-like ?-hydride can form in three equivalent $\langle 1120 \rangle$ directions (or three domains). The γ-hydride is formed as a result of either high cooling rate or long-hold at low temperature, and has a face-centered tetragonal structure. In our phase field model, this two-phase multi-domain microstructure in a single crystalline zirconium, is described by the hydrogen composition field variable $C(r, t)$ and three long range order parameters (lro) $\eta_1(r, t)$, $\eta_2(r, t)$, $\eta_3(r, t)$ to represent the three domains, where r is the spatial coordinate and t is time. While in the case of a bi-crystal, we adopted a total of six lro parameters with three in each grain to describe the different domains of hydrides.

The time evolution of these field variables is described by the time dependent Ginzburg–Landau equations [20,21] for $\eta_p(r, t)$ and the Cahn–Hilliard diffusion equation [22] for $C(r, t)$,

$$\frac{\partial \eta_P(r,t)}{\partial t} = -L_p \frac{\delta F}{\delta \eta_p(r,t)} + \varsigma_p(r,t) \tag{1}$$

$$\frac{\partial C(r,t)}{\partial t} = -M\nabla^2 \frac{\delta F}{\delta C(r,t)} + \xi(r,t) \tag{2}$$

where L and M are kinetic coefficients characterizing structural relaxation and diffusion mobility; F is the free energy of the system; $\zeta_p(r, t)$, $\xi(r, t)$ are Langivin random noise terms which are related to fluctuations in the long range order parameter and composition respectively. The noise terms satisfy Gaussian distribution and meet the requirement of the fluctuation–dissipation theorem. Since the above equations are non-linear with respect to field variables, we solve them numerically using a semi-implicit Fourier Spectral method [23].

According to thermodynamics, the equilibrium state of a multiphase system corresponds to minimum free energy. The driving force for the temporal evolution of a multiphase microstructure in single crystals consists of the following four major contributions: the reduction in chemical free energy; the decrease in the total interfacial energy between different phases; the relaxation of the strain energy caused by the lattice mismatch between the matrix and precipitates; and the reduction in the interaction energy between the eigenstrain and external load. For a bi-crystal, free energy contribution due to grain boundary should be considered.

The total chemical free energy of a multi-phase system may be expressed as [21]

$$F_c = \int_v \left[f(C(\eta_p(r)) + \sum_{p=1}^{v} \frac{\alpha_p}{2} (\nabla \eta_p(r))^2 + \frac{\beta}{2} (\nabla C)^2 \right] d^3r \tag{3}$$

where α, β are gradient energy coefficients. The integration is performed over the entire system. The first term, f (C, η_p), the local specific chemical free energy, is approximated using a Landau–type of free energy polynomial

$$\begin{aligned} f(C,\eta_p) = {} & \frac{A_1}{2}(C - C_1)^2 + \frac{A_2}{2}(C - C_2)\sum_p^v \eta_p^2 - \frac{A_3}{4}\sum_p^v \eta_p^4 \\ & + \frac{A_4}{6}\sum_p^v \eta_p^6 \\ & + A_5 \sum_{q \neq p}^{v} \eta_p^2 \eta_q^2 + A_6 \sum_{p \neq q, p \neq r}^{v} \eta_p^4 (\eta_q^2 + \eta_r^2) + A_7 \sum_{p \neq q \neq r}^{v} \eta_p^2 \eta_q^2 \eta_r^2 \end{aligned} \tag{4}$$

where v is the number of orientation variants, C_1 and C_2 are equilibrium compositions of hydrogen in matrix and in precipitate, respectively; $A_1 \sim A_7$ are phenomenological constants which are chosen to fit the local specific free energies as a function of hydrogen composition for the zirconium matrix and for the hydride. The last two terms in (3) are related to the interfacial energy between different phases.

According to Khachaturyan's theory, elastic energy can be expressed as [18]

$$\begin{aligned} E_{el} = {} & \frac{V}{2} C_{ijkl} \bar{\varepsilon}_{ij} \bar{\varepsilon}_{kl} - V C_{ijkl} \bar{\varepsilon}_{ij} \sum_p^v \varepsilon_{kl}^0(p) \overline{\eta_p^2(r)} \\ & + \frac{V}{2} C_{ijkl} \sum_p^v \sum_q^v \varepsilon_{ij}^0(p) \varepsilon_{kl}^0(q) \overline{\eta_p^2(r) \eta_q^2(r)} \\ & - \frac{1}{2} \sum_p^v \sum_q^v \int \frac{d^3g}{(2\pi)^3} B_{pq}(n) \{\eta_p^2(r)\}_g^* \{\eta_q^2(r)\} \end{aligned} \tag{5}$$

where $\overline{(...)}$ represent the volume average of (…), V is the total volume of the system, C_{ijkl} is the elastic constant tensor, $\varepsilon^0(p)$ is the stress-free transformation strain for the pth variant when $\eta_p(r) = 1$. Here we can assume $\varepsilon^0_{ij}(r) = \Sigma\varepsilon^0_{ij}(p)\eta^2_p(r)$, which denote the local stress-free transformation strain. $B_{pq}(n) = n_i\sigma_{ij}(p)\Omega_{jk}(n)\sigma_{kl}n_l$, where $\Omega_{jk}(n)$is the reverse matrix of $\Omega^{-1}_{jk} = n_i C_{ijkl}n_l$. $\boldsymbol{g}$ and $\boldsymbol{n} = \boldsymbol{g}/\mathrm{g}$ are a reciprocal vector and its unit vector in reciprocal space respectively. $\{\eta^2_q(r)\}_g$is the Fourier transform of $\eta^2_q(r)$ and $\{\eta^2_q(r)\}^*_g$ is the complex conjugate of $\{\eta^2_q(r)\}_g$.

For a bi-crystal, we assume that the grain boundary energy has the Read and Shockley's form [24,25]: in the small angle regime ($\theta < 15°$) the grain boundary energy increases with the orientation difference θ between the two grains:

$$E_b = E_0\theta(A - \ln\theta) \tag{6}$$

where E_0 and A are constants, depending on the material. In the large angle regime ($\theta \geq 15°$), the grain boundary energy is assumed to be constant. In addition, it was observed in TEM experiments that grain boundaries were often the nucleation site for the hydride [10]. We assume that, (i) there is a stronger driving force at the grain boundary region for hydride formation as compared to the bulk and this driving force is proportional to η^2_p; and (ii) once hydrides are formed at the grain boundary, the grain boundary energy E_b is minimized due to the replacement of part of the original grain boundary by hydride particles. To reflect these two assumptions, we added a free energy term only in the grain boundary region, i.e.,

$$E = E_b\left(1 - \sum\eta^2_p(r,t)\right) \text{ (at grain boundary)} \tag{7}$$

This is similar to a concept used to simulate the effect of random defects on phase transition temperature [26]. In our simulation, this grain boundary region was specified as a thin layer having a width of a few grid elements.

For bi-crystals, the simulation will include all these five contributions to the total free energy in term of the field variables, $C(r, t)$ and $?_p(r, t)$. In this work, for simplicity of the calculation, we neglect the strain energy caused by composition change of hydrogen in solid solution and all the calculation are under the homogeneous modulus approximation (i.e., the elastic constants of the precipitate phase are the same as those of the matrix).

3. Simulation results and discussion

The simulation was conducted in a 256×256 two-dimensional uniform grid with the c-axis of Zr crystal normal to the grid. In the chemical free energy term, we assume that all the parameters are the same as in our earlier work [17], which were obtained by fitting to experimental data. The elastic constants of zirconium are given in ref. [27] . A hexagonal to tetragonal transformation of γ-hydride precipitate from a single crystalline zirconium generates three possible equivalent orientation variants. The stress–free transformation strains for the first orientation domain are:

$$\begin{pmatrix} 0.551\% & 0 & 0 \\ 0 & 5.64\% & 0 \\ 0 & 0 & 5.70\% \end{pmatrix}$$

[28]. The strains for the other two orientations are obtained by rotating the first orientation domain by 120 and 240° about c-axis respectively. In this simulation, the grain boundary is a vertical line through the center of the grid. In the left hand grain, one $[11\bar{2}0]$ direction is along the horizontal axis, while in the right hand crystal one $[11\bar{2}0]$ direction has an angle θ with respect to the horizontal axis. The kinetic coefficients L_p and M in Eqs. (1) and (2) are assumed to be 0.4. The constant A in equation (6) is assumed to be 2.5 due to lack of experimental data and E_0 in equation (6) and (7) were chosen so that the surface energy of the grain boundary is in the order of 1 J/m^2. Reduced time $t^* = t/t_0$ was used to represent the aging time, where t_0 is about 10^{-7} J^{-1} L_p^{-1}. For each iteration, the time step was $\Delta t^* = 0.0008$.

At the beginning of the simulation, the value of $C_0(r, t)$ is 0.1 (atomic fraction), all $\eta_p(r, t)$ were set to zero. The two noise terms in Eq. (1) and Eq. (2) were turned on during the first 1000 time steps to mimic the local thermal fluctuations of $C(r, t)$ and $\eta_p(r, t)$.

Fig. 1 presents hydride morphology after 4000 time steps in a bi-crystal zirconium matrix for different orientation differences between the two crystals. The orientation of the right hand crystal is rotated by an angle θ with respect to the left hand crystal. It can be seen from Fig. 1 that, the density of the hydride precipitation near the grain boundary is larger than that at other places. They increase with the orientation difference between the crystals at the range of small angles, while kept constant for the large angles. We can also see that hydrides grow along habit planes with an angle about 120° from each other. The habit planes of the hydride at the right hand crystal changes with the orientation of the crystal. It is also shown that hydride precipitated in one grain will likely stop growing at the grain boundary.

Fig. 2 shows that a uniformly applied tensile strain was applied along the vertical direction with an orientation difference $\theta = 0$ between the two grains. This case is similar to single crystal simulation [17] except that some hydrides stop growth at the grain boundary. At a certain strain level, the hydrides only precipitate in the

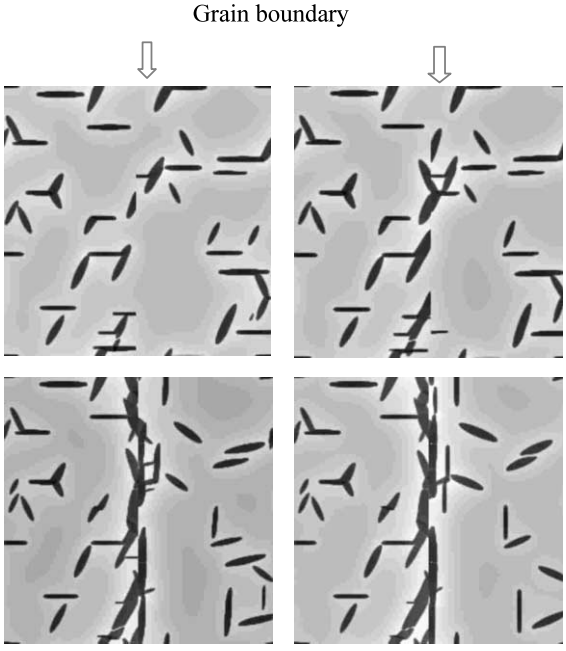

Fig. 1. Computer simulation of γ-hydride precipitation in bi-crystal at different orientation angle θ. $t^* = 4000$. (a) $\theta = 0°$; (b) $\theta = 5°$; (c) $\theta = 20°$; (d) $\theta = 30°$.

habit plane that is perpendicular to the applied strain. However, when the tensile strain was applied along the horizontal direction, hydrides prefer to precipitate and grow along [1210] and [2110] directions as shown in Fig. 3. This indicates that hydrides grow in the habit planes that are mostly close to the perpendicular direction of applied tensile load, which is in well accordance with the experimental observations.

In Fig. 4, the applied load is along the vertical direction. The [1120] direction of left hand half crystal is along the horizontal axis and that of the right hand half crystal is in an angle θ with x-axis. We can see the patterns of hydride precipitates in the right hand side changes with the angle θ. Again, hydrides prefer to grow in the habit planes that are mostly near the perpendicular direction of applied load. By comparing

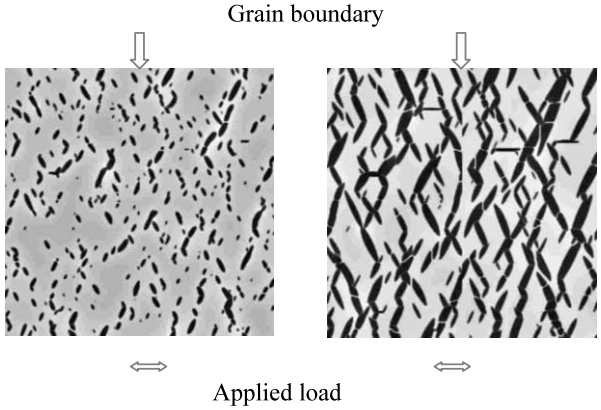

Fig. 3. γ-hydride precipitation under a tensile strain applied horizontally. $\theta = 0$, tensile strain = 0.32%. (a) $t^* = 1500$; (b) $t^* = 4000$.

all the figures, one can also notice that when there is an applied load, the grain boundary precipitation become less significant. When the load level is high, the nucleation promoted by applied load will be dominant.

4. Conclusions

By adopting a total of six lro with three lro in each grain, the hydride precipitation process in a bi-crystal system has been simulated.

The simulation result shows that nucleation density of the hydride at the grain boundary increases as compared to the bulk under the assumption in Eq. (7).

Hydrides will precipitate and grow in those habit planes that are near the perpendicular direction of the applied tensile load.

The effect of external load on hydride precipitation can be stronger than that of grain boundaries.

Acknowledgements

This work was supported by grants from the Research Grants Council of Hong Kong (B-Q411) for Shi,

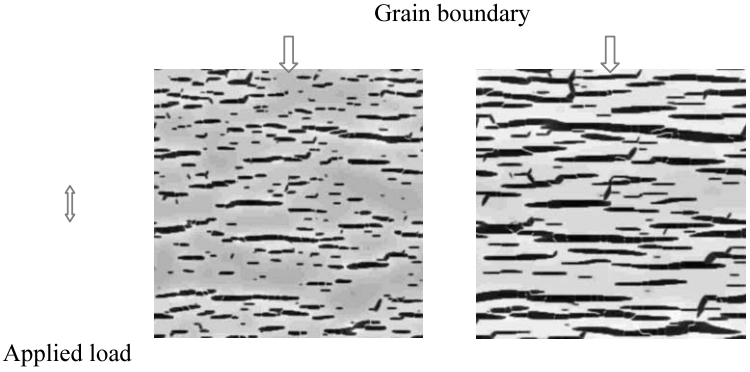

Fig. 2. Simulation of γ-hydride precipitation under a tensile strain applied vertically. $\theta = 0$, tensile strain = 0.32%. (a) $t^* = 1500$; (b) $t^* = 4000$.

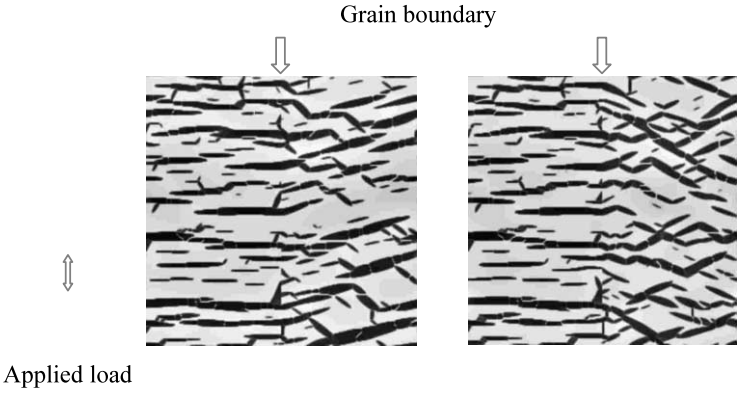

Fig. 4. γ-hydride precipitation under a tensile strain applied vertically. Tensile strain $= 0.32\%$, $t^* = 4000$; (a) $\theta = 20°$; (b) $\theta = 30°$.

Woo and Chen, and from Hong Kong Polytechnic University (G-V851) for Ma, and from the US National Science Foundation (DMR 96-33719) for Chen.

References

[1] L.Q. Chen, Y.Z. Wang, A.G. Khachaturyan, Philos. Mag. Lett. 65 (1992) 15.
[2] Y.Z. Wang, H.Y. Wang, L.Q. Chen, A.G. Khachaturyan, J. Am. Ceram. Soc. 78 (1995) 657.
[3] D. Fan, L.Q. Chen, J. Am. Ceram. Soc. 78 (1995) 769.
[4] Y. Wang, A.G. Khachaturyan, Acta Mater. 45 (1997) 759.
[5] D.Y. Li, L.Q. Chen, Acta Mater. 46 (1998) 2573.
[6] S.Q. Shi, M.P. Puls, J. Nucl. Mater. 208 (1994) 232.
[7] S. Sagat, S.-Q. Shi, M.P. Puls, Mater. Sci. Eng. A176-247 (1994) 237.
[8] S.Q. Shi, M.P. Plus, Advances in the theory of delayed hydride cracking, in: A.W. Thompson and N.R. Moody (Eds.), Hydrogen Effects in Materials, The Minerals, Metals & Materials Society, Pittsbergh, 1996, p. 611.
[9] K.S. Chan, J. Nucl. Mater. 227 (1996) 220.
[10] J.E. Bailey, Acta Metal. 11 (1963) 267.
[11] C. Roy, J.G. Jacques, J. Nucl. Mater. 31 (1969) 233.
[12] J.S. Bradbrook, G.W. Lorimer, N. Ridley, J. Nucl. Mater. 42 (1972) 142.
[13] G.P. Walters, Electrochem. Tech. 4 (1966) 216.
[14] W.J. Bayak, Trans. AIME 239 (1967) 252.
[15] R.P. Marshall, J. Nucl. Mater. 24 (1967) 34.
[16] Raabe Dierk. Computational Materials Science: The Simulation of Materials Microstructures and Properties, Weinheim, New York, 1998.
[17] X.Q. Ma, S.Q. Shi, C.H. Woo, L.Q. Chen, Comp. Mater. Sci., (2001) in press.
[18] A.G. Khachaturyan, Theory of Structural Transformations in Solids, John Wiley & Sons, New York, 1983.
[19] Artemev, Y. Wang, A.G. Khachaturyan, Acta Mater., 48 (2000) 2503.
[20] J.W. Cahn, J.E. Hilliard, J. Chem. Phys. 28 (1958) 258.
[21] Y. Wang, L.Q. Chen, A.G. Khachaturyan, J. Am. Ceram. Soc. 76 (1993) 3029.
[22] S.M. Allen, J.W. Cahn, Acta Metal. 27 (1979) 1085.
[23] L.Q. Chen, J. Shen, Comput. Phys. Commun. 108 (1998) 147.
[24] W. Shockley, W.T. Read, Phys. Rev. 75 (1949) 692.
[25] W.T. Read, W. Shockley, Phys. Rev. 78 (1950) 275.
[26] S. Semenovskaya, A.G. Khachaturyan, Acta Mater. 45 (1997) 4367.
[27] M. Lgarashi, Phil. Mag. B 63 (1991) 603.
[28] G.J.C. Carpenter, J. Nucl. Mater. 48 (1973) 264.